

**Titel/Title:** How solvent-free crosslinking conditions alter the chemistry and topology of hemiketal based polymer networks

**Autor\*innen/Author(s):** Tobias Urbaniak, Katrin Greta Hoffmann, Matthias Herrera Glomm, Hartmut Oschkinat, Peter Schmieder, Katharina Koschek

Veröffentlichungsversion/Published version: Postprint

Publikationsform/Type of publication: Artikel/Aufsatz

**Empfohlene Zitierung/Recommended citation:**

Tobias Urbaniak, Katrin Greta Hoffmann, Matthias Herrera Glomm, Hartmut Oschkinat, Peter Schmieder, Katharina Koschek, 2021, How solvent-free crosslinking conditions alter the chemistry and topology of hemiketal based polymer networks, *Polymer*, 229, p. 123986, <https://doi.org/10.1016/j.polymer.2021.123986>.

**Verfügbar unter/Available at:**

(wenn vorhanden, bitte den DOI angeben/please provide the DOI if available)

<https://doi.org/10.1016/j.polymer.2021.123986>

**Zusätzliche Informationen/Additional information:**

Accepted for publication.

Corresponding author:

Katharina Koschek, Fraunhofer Institute for Manufacturing Technology and Advanced Materials (IFAM), Bremen, Germany

[katharina.koschek@ifam.fraunhofer.de](mailto:katharina.koschek@ifam.fraunhofer.de)

# How solvent-free crosslinking conditions alter the chemistry and topology of hemiketal based polymer networks

Tobias Urbaniak<sup>a,b</sup>, Katrin Greta Hoffmann<sup>b</sup>, Matthias Herrera Glomm<sup>c</sup>, Hartmut Oschkinat<sup>c</sup>, Peter Schmieder<sup>c</sup>, Katharina Koschek<sup>b,\*</sup>

<sup>a</sup> University of Bremen, Chemical Department, Leobener Straße 3, 28359, Bremen, Germany

<sup>b</sup> Fraunhofer Institute for Manufacturing Technology and Advanced Materials (IFAM), Wiener Strasse 12, D-28359, Bremen, Germany

<sup>c</sup> Leibniz-Forschungsinstitut für Molekulare Pharmakologie (FMP), Campus Berlin-Buch, Robert-Roessle-Str. 10, 13125, Berlin, Germany

## A B S T R A C T

### Keywords:

Dissociative polymer networks

Self-healing

Responsiveness

A solvent free reaction of PCL based polyester polyols with a crosslinking molecule based on a vicinal tricarbonyl results covalent adaptable polymer networks that differ in their thermal behavior, swelling, and solubility properties. Mild processing results polymer networks based on hemiketal/ketone equilibrium with properties typical for dissociative networks including dissolution in presence of water or elevated temperature and self-healing properties. Further thermal treatment of the polymer entails changes in swelling, and solubility properties. Constant glass transition temperatures of the differently treated polymers indicate a steady overall network density, but changes in the nature of the network structure. By varying the number of OH-groups, molar mass and stoichiometric ratio of the polyester polyol and the crosslinking molecule, respectively, material properties can be adjusted. This approach gives access to reversibly crosslinked polymers varying in their responsiveness and overall mechanical properties.

## 1. Introduction

Polymers based on reversible chemical bonds can be responsive to external stimuli and can therefore adapt to desired properties depending on external factors such as temperature and pressure. Using dynamic covalent chemistry (DCC) thermosetting smart materials can be developed responding to their environment. Different stimuli can be used to achieve changes in the polymer constitution or crosslinking stage through the use of dynamic covalent chemistry [1]. Polymer networks based on DCC are collectively called covalent adaptive networks (CAN) [2–4]. Depending on the mechanism type of DCC reaction, associative versus dissociative polymer networks can be distinguished [5].

In associative networks, kinetically controlled exchange reactions of bond-forming and bond-breaking reactions take place simultaneously. This ensures that the average number of network points in the polymer and thus the network density remains equal maintaining its network integrity over the entire temperature range [4,6]. If the bond exchange is sufficiently fast, CANs show viscoelastic behavior with rapid relaxation properties being able to flow due to the influence of external load [5,6].

In contrast, dissociative CAN show thermodynamically controlled reversible condensation and addition reactions. A shift in equilibrium is responsible for the dynamic behavior. An environmental change e.g. temperature increase, shifts the equilibrium to the dissociated state, which entails a decrease in network density followed by a sharp drop in viscosity [5,6]. This results in topological rearrangements through flow and stress relaxation. Further environmental changes, e.g. temperature decrease, shift back the equilibrium of the reversible chemical reaction rebuilding the network and regaining original properties [5,6]. Dynamic covalent chemistry provides materials with unique properties and opens up new opportunities for manufacturing, repair and recycling of CAN based thermosetting materials.

Various reversible reactions were studied and used in terms of DCC, e.g., Diels–Alder reaction [7,8], vinylogous urethane/urea [5,9,10] disulfide exchange [11–13], imine formation [14–18] or reversible ring-opening of benzoxazine [19,20]. Among them, the reversible hemiketal reaction [21,22] is gaining more and more interest in DCC and was described by the group of T. Endo who has performed preliminary work on the reversibility of the reaction of 1,

\* Corresponding author.

E-mail addresses: [tobias.urbanik@ifam.fraunhofer.de](mailto:tobias.urbanik@ifam.fraunhofer.de) (T. Urbaniak), [katrin.hoffmann@empa.ch](mailto:katrin.hoffmann@empa.ch) (K.G. Hoffmann), [hiller@fmp-berlin.de](mailto:hiller@fmp-berlin.de) (M.H. Glomm), [oschkinat@fmp-berlin.de](mailto:oschkinat@fmp-berlin.de) (H. Oschkinat), [schmieder@fmp-berlin.de](mailto:schmieder@fmp-berlin.de) (P. Schmieder), [katharina.koschek@ifam.fraunhofer.de](mailto:katharina.koschek@ifam.fraunhofer.de) (K. Koschek).

3-diphenylpropanetrione with alcohols and water [23,24]. Vicinal tricarbonyl compounds are known to react with various nucleophiles such as water [24,25] and alcohols [24] without the need of catalyst due to the highly electrophilic nature of the three adjacent carbonyl groups. Furthermore, they react with thiols [26] or amines [27] forming hemithioketals and amins, respectively. The formed hemiketal bonds are able to exchange with water representing a reversible switch. T. Endo et al. used the 3,3-(1,4-phenylene)bis(1-phenylpropane-1,2,3-trione) (bistriketone) to crosslink a poly(vinyl alcohol) and poly(2-hydroxyethyl methacrylate) in a solvent-based reaction to an insoluble material that could be dissolved again in water due to decrosslinking. The crosslinking molecule bistriketone was recovered up to 58% after separation and a drying step [28]. Another recent work by Nakagawa et al. presented a solvent-based crosslinking of a vicinal tricarbonyl-functionalized vinyl based polymer with 1,12-dodecanediol as a crosslinking molecule. The reaction yielded a solid that could be repaired in a solvent-assisted self-healing using water or methanol after cutting the polymer in pieces. They proposed that the addition of methanol affects the physical and chemical polymer constitution due to a decreased crosslinking density and a shift of the equilibrium to the decrosslinked state [29]. Until now, the ketone/hemiketal chemistry was studied in solvent based set-ups solely.

This contribution elucidates the impact of a solvent-free environment and processing conditions, e.g. temperature and reaction time on the CAN formation by a reversible crosslinking between a bistriketone as a crosslinking molecule and multifunctional poly( $\epsilon$ -caprolactone) (PCL) based polyester polyols. We could show that the reaction conditions affect the chemistry of the polymer network, which seem to affect the dissociative nature of the polymer network. Depending on the polymer nature, the material's behavior changes significantly. Various polyester polyols were studied with respect to the number of available OH-groups, the molar mass and the stoichiometry ratio of bistriketone and PCL. Depending on the reaction pathway, the final products differed in their mechanical as well as dynamic properties.

## 2. Materials and methods

### 2.1. Materials in experiments

Dimethylsulfoxide- $d_6$  (DMSO- $d_6$ ) was purchased from Deutero (Kastellaun, Germany) and was dried over molecular sieve 4 Å. NaH (60% in oil) was purchased from Sigma Aldrich (Darmstadt, Germany) and washed with tetrahydrofuran (THF) (anhydrous) before use. Dimethyl terephthalate, acetophenone, toluene dimethylsulfoxide, *N*-bromosuccinimide (NBS), *n*-butylamine, 1-butanethiol, 4-nitrophenol, 1-butanol, acetone (SeccoSolv) and poly(ethylene oxide) 400 g/mol, were purchased from Sigma Aldrich (Darmstadt, Germany) and 4-nitrothiophenol, 4-nitroaniline were purchased from TCI (Eschborn, Germany) and used as received. Used polyester polyols are depicted in Table 1.

### 2.2. Syntheses procedures

The crosslinking molecule 3,3-(1,4-Phenylene)bis(1-phenylpropane-1,2,3-trione) (bistriketone (**3**)) was synthesized based on the procedures as described by T. Endo et al. [30]. The single steps are described briefly.

#### 2.2.1. 3,3-(1,4-Phenylene)bis(1-phenylpropane-1,3-dione) (**1**)

NaH 60% in mineral oil (8.00 g, 200 mmol) was washed with dry THF (2 x 20 mL). To a suspension of NaH in dry THF (100 mL), acetophenone (11.7 mL, 12.01 g, 100 mmol) and dimethyl terephthalate (9.70 g, 50.0 mmol) and were added and mixed at ambient temperature for 60 min and at 50 °C for 48 h under  $N_2$  atmosphere. The mixture was cooled to ambient temperature and quenched by the addition of water (200 mL) and aqueous HCl (2 M, 100 mL). The suspension was filtered

**Table 1**

Used polyester polyols received from Perstorp (Warrington, United Kingdom) were dried in vacuum at 110 °C for 1h before use.

2-oxepanone, polymer with:	Product name	Molar mass	Acronym
2,2-dimethyl-1,3-propanediol	Capa™ 2100	1000	diPCL1000
2-ethyl-2-(hydroxymethyl)-1,3-propanediol	Capa™ 3031	300	triPCL300
2-ethyl-2-(hydroxymethyl)-1,3-propanediol	Capa™ 3041	425	triPCL425
2-ethyl-2-(hydroxymethyl)-1,3-propanediol	Capa™ 3050	540	triPCL540
2-ethyl-2-(hydroxymethyl)-1,3-propanediol	Capa™ 3091	900	triPCL900
2-ethyl-2-(hydroxymethyl)-1,3-propanediol	Capa™ 3201	2000	triPCL2000
2,2 bis(hydroxymethyl)-1,3-propanediol	Capa™ 4101	1000	tetraPCL1000
2,2-dimethyl-1,3-propanediol	Capa™ 2043	400	diPCL400

and the collected solid was washed with water and chloroform, and dried in vacuum to yield **1** as a light yellow solid (16.4 g, 44.3 mmol, 89%).

$^1H$  NMR (200 MHz,  $CDCl_3$ , (enol)):  $\delta$  16.81 (s, 2H, O-H), 8.10 (s, 4H, Ar-H), 8.02 (d, 4H  $J$  = 8.0 Hz, Ar-H), 7.47–7.61 (m, 6H, Ar-H) 6.92 (s, 1H, C=C-H) ppm.

#### 2.2.2. 3,3-(1,4-Phenylene)bis(2,2-dihydroxy-1-phenylpropane-1,3-dione) (bis(gem-diol) (**2**))

3,3-(1,4-Phenylene)bis(1-phenylpropane-1,3-dione) (**1**) (9.00 g, 24.6 mmol) and NBS (8.75g, 49.2 mmol) were stirred in DMSO (dry) (250 mL) at 60 °C for 24 h. Distilled water (50 mL) was added after cooling the mixture to ambient temperature. The solution was stirred for 1 h. After the addition of water (250 mL) the product precipitated and the resultant suspension was filtered. The collected solid was washed with water and chloroform yielding **2** as a white solid.

$^1H$  NMR (200 MHz, DMSO- $d_6$ ):  $\delta$  8.04 (s, 4H, Ar-H), 8.01-7.96 (m, 4H, Ar-H), 7.64-7.42 (m, 6H, Ar-H) ppm.

#### 2.2.3. 3,3-(1,4-Phenylene)bis(1-phenylpropane-1,2,3-trione) (bistriketone (**3**))

3,3-(1,4-Phenylene)bis(2,2-dihydroxy-1-phenylpropane-1,3-dione) **2** was dried in vacuum by heating at 100 °C for 4 h to give **3** as an orange solid; mp: 130.0 °C. (6.31 g, 15.8 mmol, 65%)

$^1H$  NMR (200 MHz, DMSO- $d_6$ ):  $\delta$  8.33 (s, 4H, Ar-H), 8.13 (4H, d  $J$  = 7.31, Ar-H), 7.85 (2H, t,  $J$  = 7.30 Hz Ar-H), 7.67 (4H, t,  $J$  = 7.53) ppm.  $^{13}C$  { $^1H$ } NMR (125 MHz, DMSO- $d_6$ ):  $\delta$  191.3, 189.9, 187.1, 136.3, 135.7, 131.7, 130.4, 130.0, 129.3 ppm. HRMS (ESI,  $m/z$ ):  $[M]^+$  calcd for  $C_{24}H_{14}O_6$ , 398.07849; found, 398.07880.

### 2.3. General procedures for the reaction of bistriketone **3** with polyester polyols

The reaction between **3** and PCL is a continuous reaction between processing stages. After the individual processing condition, the cross-linked polymer has different material properties.

Processing condition I: The appropriate polyester polyol and **3** were placed in a mortar and homogenized. The resulting paste was heated up to 130 °C remaining at that temperature for 5 min (Table 1, Table 2).

Processing condition II: The appropriate polyester polyol and **3** were placed in a mortar and homogenized. The resulting paste was heated up to 130 °C and kept at that temperature for 180 min (Table 1, Table 2).

Processing condition III: The appropriate polyester polyol and **3** were placed in a mortar and homogenized. The resulting paste was heated up to 130 °C and kept at that temperature for 180 min. Afterwards the material was heated to 180 °C and kept at that temperature for 180 min

**Table 2**

Amount of PCL and PEO, which were used for the processing condition I, II and III. 0.100 g of **3** were used for each reaction.

Product	PCL/PEO	$M_n/g^{\circ}\text{mol}^{-1}$	OH-groups	m(PCL, PEO)/g
3-diPCL1000	diPCL1000	1000	2	0.251
3-triPCL300	triPCL300	300	3	0.050
3-triPCL425	triPCL425	425	3	0.071
3-triPCL540	triPCL540	540	3	0.090
3-triPCL900	triPCL900	900	3	0.151
3-triPCL2000	triPCL2000	2000	3	0.335
3-tetraPCL1000	tetraPCL1000	1000	4	0.126
3-diPEO400	diPEO400	400	2	0.101
3-diPCL400	diPCL400	400	2	0.101

(Table 1, Table 2).

Preparation of the self-healing tests specimens: tetraPCL1000 (0.984 g) and **3** (0.800 g) were placed in a mortar and homogenized. The resulting paste was transferred in a silicon dog bone shaped mold that was preheated to 130 °C for 10 min in a vacuum oven. Filled silicon forms were heated up to 130 °C for 10 min, and vacuum was applied for degassing as soon as the paste became liquid. In case gas bubbles were still present after degassing, they were removed with the help of a thin cannula. Specimens were tempered for 10 min at 80 °C in an oven and cooled down to room temperature in a dry desiccator. Specimen dimensions are according to DIN EN ISO 20753:2017 type A14 with an overall length of 50 mm, a thickness of 1 mm a narrow parallel-sided section with a length of 20 mm and width of 2.5 mm.

Preparation of the DMA test specimen: The polymer network 3-tetraPCL1000-I was hold for 7 h at 130 °C in a silicone mold with dimensions of 3.5 cm × 1.0 cm × 0.3 cm to get specimen of the polymer network 3-tetraPCL1000-II. The polymer network 3-tetraPCL1000-II was additionally heated to 180 °C and kept for 3 h at 180 °C yielding 3-tetraPCL1000-III.

#### 2.4. Methods

NMR spectroscopy:  $^1\text{H}$  NMR spectra were recorded at 200 MHz, on a DPX-200 Advance NMR spectrometer from Bruker (Rheinstetten, Germany).  $^{13}\text{C}$  NMR spectra were recorded at 125 MHz on a Bruker AVANCE III 500 spectrometer (Rheinstetten, Germany). For 2D- NMR analysis  $^1\text{H}$  and  $^{13}\text{C}$  NMR spectra, as well as the correlated HMBC and HMQC spectra were recorded on a 600 MHz and 150 MHz Bruker Ultra-Shielded-Plus (AV III Cabinet). In case of DMSO- $d_6$  and  $\text{CDCl}_3$  residual protons were used as internal standard.

Solid-state MAS NMR measurements were carried out on a 400 MHz WB spectrometer (Bruker Biospin GmbH) equipped with a 4 mm MAS probe head at a sample temperature of 20.4 °C and a rotation speed of 10 kHz. All spectra were indirectly referenced to the proton frequency of the methyl group of 2,2-dimethyl-2-silapentane-5-sulfonate (DSS) (0 ppm). Additionally, the sample temperature was indirectly measured using a  $\text{H}_2\text{O}$ -DSS sample [31]. The experimental conditions for the cross polarization (CP) experiments were optimized with a  $^{13}\text{C}$ -labeled glycine sample [32]. The energy for the initial proton excitation pulse was optimized to a value at which the pulse length was 2.5  $\mu\text{s}$  (100 kHz). For  $^{13}\text{C}$  NMR measurements, the energy of the excitation pulse was optimized to a pulse length of 5  $\mu\text{s}$  (50 kHz). The magnetization transfer (cross polarization (CP)) between  $^1\text{H}$  and  $^{13}\text{C}$  was carried out with a power of 80 kHz ( $^1\text{H}$ ) and 54 kHz ( $^{13}\text{C}$ ) and a ramp of 75–100% (on the 1H channel) for a duration of 1.5 ms. During the acquisition, protons were decoupled with a pulse power of 100 kHz (SPINAL 64 decoupling sequence) [33]. 5 to 10 experiments, with a number of scans of 1024 and a recycle delay of 5 s were recorded for each sample and subsequently summed up with the Bruker software Topspin 4.03 (Bruker BioSpin GmbH).

Infrared spectroscopy was conducted on a Bruker Equinox 55 FTIR spectrometer with a golden gate ATR unit and a Bruker Vertex70 FTIR

spectrometer with a heatable platinum ATR A225/Q-DLST unit at 23 °C or 80 °C. The absorption was measured in a range from 650 to 4000  $\text{cm}^{-1}$  with a resolution of  $\pm 4 \text{ cm}^{-1}$  and 32 scans. The absorption bands are given in wavenumbers ( $\text{cm}^{-1}$ ).

High-resolution mass spectra were recorded on a MAT 95 XL, EI 70 eV.

Thermoanalytical measurements: Glass transition ( $T_g$ ) and melting temperature ( $T_m$ ) measurements were performed on a thermal analyzer Q-Series TA Instruments (New Castle, DE, USA) from  $-90 \text{ }^\circ\text{C}$  to  $300 \text{ }^\circ\text{C}$  at a heating rate of  $10 \text{ K}\cdot\text{min}^{-1}$ . Melting points were determined as the peak temperature and  $T_g$ s as the turning point of the endothermic signal using the tangent method (Table S 01, Supporting Information).

Thermogravimetric analysis (TGA) was performed on TA Instruments Q5000 IR (New Castle, DE, USA) from 30 to 800 °C with  $10 \text{ K}\cdot\text{min}^{-1}$  with an aluminum pan under a  $25 \text{ mL min}^{-1} \text{ N}_2$ -flow (Table S 02, Figure S 20 Supporting Information).

Dynamic mechanical analyses (DMA) were carried out in single cantilever mode with the DMA 2980 from TA Instruments according to the parameters  $-100 \text{ }^\circ\text{C}$  to  $+100 \text{ }^\circ\text{C}$ ,  $10 \text{ Hz}$   $2 \text{ K}\cdot\text{min}^{-1}$  in case of the polymer network 3-tetraPCL1000-II and  $-100 \text{ }^\circ\text{C}$  to  $+180 \text{ }^\circ\text{C}$ ,  $10 \text{ Hz}$   $2 \text{ K}\cdot\text{min}^{-1}$  in case of the polymer network 3-tetraPCL1000-III (Fig. 21 Supporting Information).

Rheology experiments were performed on the ARES rheometer (Rheometric Scientific) with an LN2 cooling unit in a plate-plate geometry (25 mm plates). The polymer network 3-tetraPCL1000-I was liquefied at 130 °C and set to a gap of 200  $\mu\text{m}$ . During the measurement, the storage and loss modulus were determined oscillatory at 1 Hz. The deformation of the sample was automatically adjusted to the viscosity of the sample during the measurement. The cooling rate was measured at  $5 \text{ K}\cdot\text{min}^{-1}$  from 130 to 0 °C. The crosslinking reaction was followed isothermally at 130 °C for 300 min. During the measurement, the storage and loss modulus were determined oscillatory at 1 Hz.

X-ray diffraction experiments were carried out on the MiniFlex600 diffractometer (Rigaku) with a Bragg-Brentano geometry and a Cu ( $K\alpha$ ) source in the range of  $10\text{--}60^\circ 2\theta$  and a step size of  $0.0175^\circ 2\theta$ .

Gel content was determined by performing a continuous soxhlet extraction under reflux with 100 mL acetone and acetone/water 9:1 for 24 h, respectively. Acetone and water were used for the extraction because both starting materials dissolve very well in acetone and the exchange reaction between the geminal diol to the carbonyl group and the alcohol triggers with water. Samples were weighed before soxhlet extraction (m0). After extraction, the residue in the flask was vacuum dried with a rotary evaporator and in a vacuum oven (50 °C, <100 mbar) until constant weight (mR). Solid parts were dried in a vacuum oven (50 °C, <100 mbar) until constant weight. The gel content was calculated as follows (Equation (1)):

$$\text{gel content (\%)} = (1 - mR/m0) \times 100\% \quad (1)$$

Swelling ratio was determined based on DIN EN ISO 175. Each sample was weighed before (m(dry)) and after (m(swollen)) swelling in dry acetone and acetone with  $\text{H}_2\text{O}$  9:1 for 24 h.

The swelling ratio was calculated as (Equation (2)):

$$\text{Swelling ratio \%} = \frac{m_{\text{swollen}} - m_{\text{dry}}}{m_{\text{dry}}} \times 100\% \quad (2)$$

The conditioning of the polymer network 3-tetraPCL1000-I at high humidity was carried out for 24 h in a hermetically sealed box with saturated NaCl solution with a relative humidity of 72% at 23 °C. For dry conditioning, polymer network 3-tetraPCL1000-I was stored in a desiccator with silica gel as a desiccant for 24 h.

Tensile tests were performed on the basis of DIN EN ISO 527-1:2016 and 527-2:2012 with a universal testing machine (Zwick Roell AG, Ulm, DE), maximum force 100 kN) and a 200 N load cell at 23 °C 50% relative humidity. The clamping length was 27 mm, the pre-load 0.05 N and testing speed 200 mm/min. The traverse displacement was used to calculate the strain. The tensile modulus was calculated at linear strain

between 0.5% and 1.0%

### 2.5. Performance of dissolving and self-healing experiments

Reactive solvent experiments: Rod-shaped samples were prepared by manufacturing 3-tetraPCL1000-II based on general procedure II at 130 °C for 7 h in the oven. All samples were initially charged with 2 ml of N-methyl-2-pyrrolidone (NMP) in rolled-edge glasses and treated with 0.2 ml of each nucleophile, respectively: *n*-butylamine, 1-butanethiol, 1-butanol, 4-nitroaniline 4-nitrothiophenol, 4-nitrophenol or water. Subsequently, the exchange reaction and the associated depolymerization after 24 h at 23 °C were visually investigated.

Self-healing experiments: Specimens were stored at all times in dry desiccator at 23 °C. A first tensile testing yielded the virgin tensile properties of the material. Broken specimens were placed back into silicon molds and the location of the fracture was recorded. The area of fracture was heated from below to 130 °C with help of a heating element for 6 min while being covered from above with a small aluminum cap. The heated part of the sample liquefied, changed the color from orange to red with a subsequent closing of the gap. The healed specimens were cooled down to room temperature in a dry desiccator. After 24 h the tensile test was repeated to determine the tensile properties after the healing event. In total, two self-healing cycles with following tensile testing were performed.

## 3. Results and discussion

Bistriketone (**3**) was used as crosslinking molecule in order to study the crosslinking and decrosslinking reactions with multifunctional poly( $\epsilon$ -caprolactone) (PCL) based polyester polyols in dependence of varying processing conditions. In contrast to the described solvent-based procedures by T. Endo and S. Nakagawa [28–30], the crosslinking reactions of the bistriketone **3** with a tetrafunctional poly( $\epsilon$ -caprolactone) (tetraPCL1000) were conducted in bulk yielding a crosslinked polymer **4** (Fig. 1). However, variations in the applied processing conditions regarding reaction time and temperature proved to affect the resulting material.

Therefore, equimolar mixtures of bistriketone **3** with tetraPCL1000 were applied to three processing conditions, namely, 5 min heating at 130 °C (condition I), 3 h heating at 130 °C (condition II), and 3 h heating at 130 °C and 180 °C, (condition III), respectively.

DSC curves of the resulting crosslinked polyesters 3-tetraPCL1000-I, -II and III revealed a  $T_g$  around 10 °C for all three polymers (Fig. 2, left). In comparison to the starting material tetraPCL1000 ( $T_g = -65$  °C) the higher  $T_g$  of all studied polymeric materials proved a successful formation of oligomeric or polymeric structures.

In the course of 3-tetraPCL1000-I curve, an endothermic event around 70 °C that was assigned a liquefaction of the polymer after bond breaking of the hemiketal sites rather than a melting of crystallites. Melting and crystallization was excluded performing XRD measurements (Figure S 05, Supporting Information). The endothermic signal was missing for 3-tetraPCL1000-II and 3-tetraPCL1000-III indicating

that the polymers did not liquefy after further processing. Exothermic signals at 230 °C were noted solely for the polymers 3-tetraPCL1000-I and II with an enthalpy drop from 148 to 85 J/g with increasing processing time changing from processing condition I to II. That effect was studied in more detail by isothermal rheology that showed a gel point after 150 min at 130 °C pointing to sequential reactions or rearrangements and a transformation from a viscous to a visco-elastic properties (Fig. 2, right). Thus, the nature of the polymer network changes throughout the processing.

The overall temperature dependent material properties of the two polymer networks 3-tetraPCL1000-II and 3-tetraPCL1000-III, were examined using dynamic-mechanical analysis (DMA) (Fig. 3 and Figure S 21, Supporting Information).

The DMA measurements showed a one-stage drop in the storage modulus with increasing temperature. For the polymers 3-tetraPCL1000-II and 3-tetraPCL1000-III,  $T_g$  of 15 and 11 °C were determined at the peak maximum of the loss module, respectively. The polymer 3-tetraPCL1000-III, which was additionally treated at 180 °C, exhibited a higher storage modulus compared to 3-tetraPCL1000-II at  $-100$  °C. This indicates a reduced segment mobility within the polymer network after reaching processing step III at low temperatures.

### 3.1. Impact of processing on polymer network properties

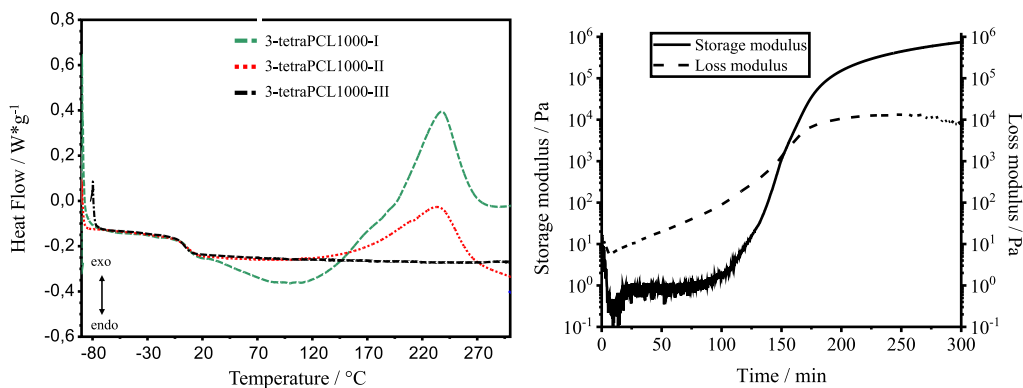
With the aim to elucidate structural changes during the three processing conditions, FT-IR and solid state  $^{13}\text{C}$  NMR experiments were performed. When comparing the IR spectra, the overlap of carbonyl and hydroxyl bands prevents a distinct separation of the single species. IR bands at 1723, 1676 and 1652  $\text{cm}^{-1}$  were assigned to the bistriketone whereas the band at 1723  $\text{cm}^{-1}$  corresponding to the centered carbonyl group overlaps with PCL's carbonyl group (Figure S 06, Supporting Information). Differences in the polymer stages after the various processing conditions appeared solely in a carbonyl band shift from 1681 to 1723  $\text{cm}^{-1}$  during conversion throughout the processes I to III (Fig. 4). The shift of the carbonyl band to higher wavenumbers indicates a diminishing bond distance and thus a stronger bond between the oxygen and the carbon atom as it could be found, e.g. in ester functionalities. Furthermore, the hydroxyl band disappeared almost completely in the polymer network after processing condition III (3-tetraPCL1000-III).

Solid state  $^{13}\text{C}$  NMR showed in the case of the crosslinking molecule bistriketone **3** chemical shifts for the three carbonyl groups at  $\delta = 195.8$ , 190.9 and 187.7 ppm. The aromatic carbon atoms appeared at  $\delta = 138.8$ –128.5 ppm (Fig. 5).

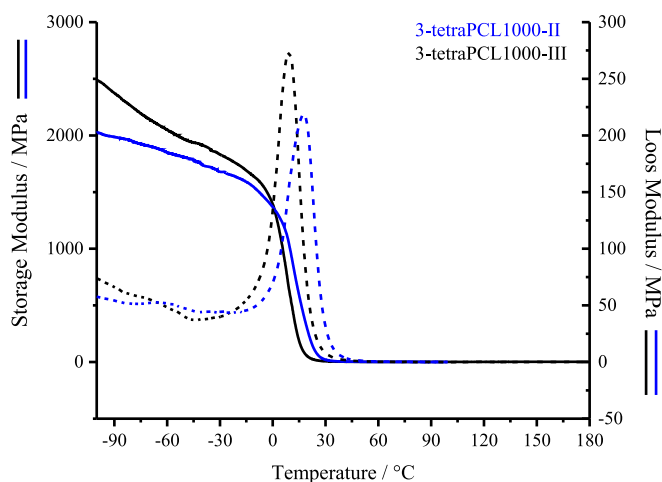
3-tetraPCL1000-I isolated after 5 min at 130 °C showed carbonyl groups and the aromatic signals of bistriketone **3**. Moreover, the sample after the first processing condition proved to contain signals corresponding to PCLs carbonyl ( $\delta = 175.2$  ppm) and aliphatic groups (ranging from  $\delta = 69.6$  ppm to  $\delta = 23.0$  ppm). An additional signal was observed at a chemical shift of  $\delta = 102.3$  ppm that was assigned to a hemiketal carbon atom. That demonstrated and proofs that the hemiketal bonds are being formed in processing condition I and cause the crosslinking in solid state.



Fig. 1. Reaction between **3** and PCL to the hemiketal product **4**.



**Fig. 2.** Left: DSC thermogram of the crosslinked material 3-tetraPCL1000 after processing condition I (3-tetraPCL1000-I), II (3-tetraPCL1000-II) and III (3-tetraPCL1000-III). Right: Isothermal rheology measurement at 130 °C of the crosslinking reaction of bistriketone **3** with tetraPCL1000 in processing condition II.



**Fig. 3.** DMA measurement of 3-tetraPCL1000-II and of 3-tetraPCL1000-III.

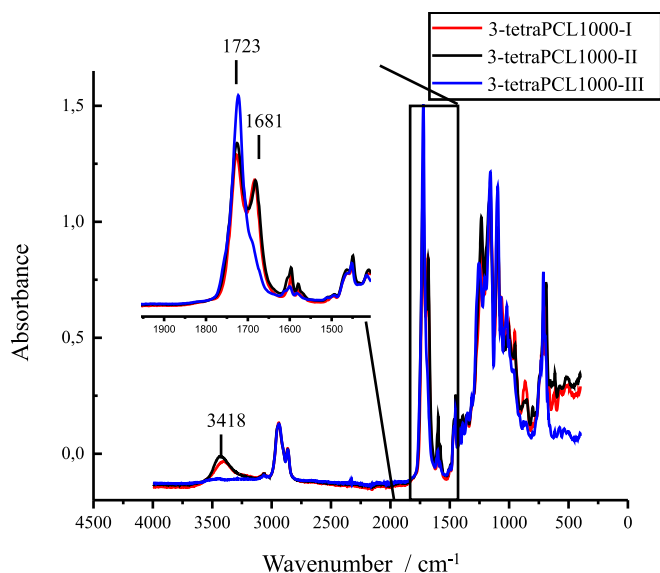


**Fig. 4.** IR spectroscopic examination of the three polymer networks after processing conditions I, II, and III.

During the conversion from 3-tetraPCL1000-I to 3-tetraPCL1000-II and 3-tetraPCL1000-III the signal intensity corresponding to the carbon signal of hemiketal ( $\delta = 102.3$  ppm) bond decreased, whereas a new signal appeared at  $\delta = 87.3$  ppm and  $\delta = 77.2$  ppm for 3-tetraPCL1000-II and 3-tetraPCL1000-III, respectively. Furthermore, additional signals were observed in the range of  $\delta = 171.8$  ppm and  $\delta = 165.8$  ppm corresponding to the region of ester carbonyl groups for both processing condition II and III. The conversion of the polymer network 3-tetraPCL1000-I into the polymer network 3-tetraPCL1000-III is believed to be a continuous process that passes over the second processing stage 3-tetraPCL1000-II. In order to proof this, the reaction between the bistriketone **3** and a dihydroxyl PCL (diPCL400) was performed to confirm the signal assignment in the solid state NMR measurement. The single NMR Spectra are shown in Figs. S8–13 in Supporting Information. Correlation of the  $^{13}\text{C}$  and  $^1\text{H}$  spectra revealed a  $^3J$  coupling between the protons of the methylene group (c) of diPCL400 and the  $\text{sp}^3$ -hybridized carbon (j) of bistriketone (Fig. 6). This coupling clearly confirms the existence of the hemiketal after processing condition I. In solution NMR spectra of 3-diPCL400-II resulting from the processing condition II, an analogue signal at 87 ppm was observed. Based on HMQC and HMBC NMR experiments (SI Figure S 10) the corresponding carbon atom was assigned a quaternary atom in the direct neighborhood of an aromatic moiety. For 3-diPCL400-III additional signals can be seen in the  $^1\text{H}$  NMR spectrum at the chemical shift  $\delta = 6.3$  ppm (SI Figure S 11). This shift range indicates alkene hydrogen atoms. In 2D NMR HMQC experiments hydrogen atoms with the chemical shift  $\delta = 6.3$  ppm could be assigned to the carbon atom at the chemical shift  $\delta = 74$  ppm (SI Figure S 13). Both signals were observed for the first time in the NMR spectra after processing condition III. Moreover, those signals showed a correlation to the carbonyl groups and the aromatic protons in the HMBC experiment. With a correlation of the hydrogen atom  $\delta = 6.3$  ppm to a carbon atom with a chemical shift of  $\delta = 74$  ppm, and a  $\text{sp}^3$  hybridization, the assumed alkene type structure must be excluded and a different type of bond assumed. Additional signals at  $\delta = 170$  and 163 ppm for 3-diPCL400-II and 3-diPCL400-III, respectively, could be assigned to ester motifs confirming the observation and assignment of solid state NMR experiments.

In sum, neither FT-IR nor NMR measurements revealed the full understanding of the polymer structure changing throughout the processing conditions. However, both experimental set-ups suggested the additional carbonyl groups 3-tetraPCL1000-III and 3-diPCL400-III to belong to ester-like bonding motifs.

Thermogravimetric analysis confirmed the potential structural changes entailing difference in thermal stabilities of the polymers at the three processing conditions (Fig. 7). Under nitrogen, the temperatures at maximum mass loss were in the same range for the three polymer networks (3-tetraPCL1000-I = 401 °C; II = 409 °C, III = 404 °C), and

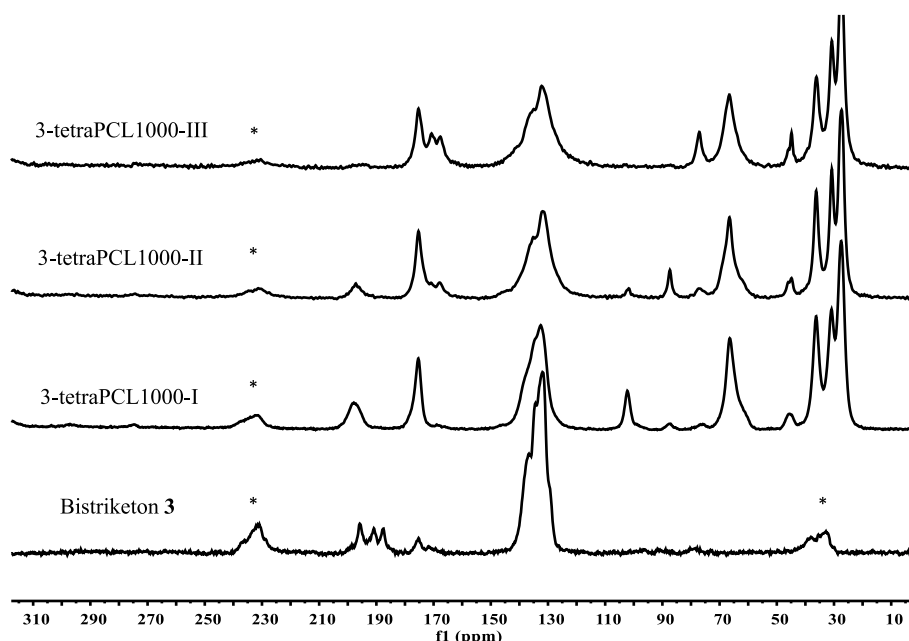


Fig. 5. Solid-state NMR measurements of the three polymer networks after processing conditions I, II, III and bistriketone **3** (\* indicates the rotation sidebands).

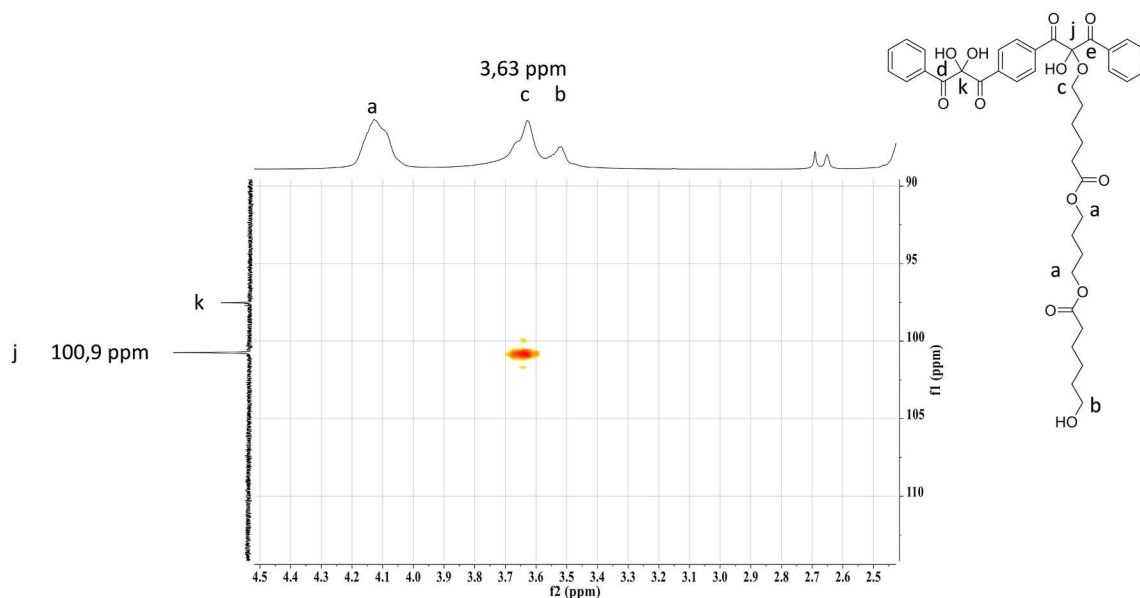


Fig. 6. HMBC spectrum of the oligomer 3-diPCL400-I in DMSO- $d_6$ .

slightly higher in comparison to the neat PCL (tetraPCL1000 = 393 °C) and the crosslinking agent bistriketone **3** (346 °C). However,  $T_{1\%}$  and  $T_{5\%}$  values of 3-tetraPCL1000-I proved to be lower than the starting material tetraPCL1000 ( $T_{5\%} = 291$  °C) and much lower in comparison to 3-tetraPCL1000-III (e.g.  $T_{5\%} = 221$  °C versus 343 °C, Table S 02, Supporting Information). The large temperature difference up to a mass loss of 10% between the polymers processed by I and III points to a much more labile network structure of 3-tetraPCL1000-I. T. Endo observed similar low thermal stabilities in acrylate networks based on hemiketal linkages. He attributed the premature mass loss to the decomposition of the thermally labile hemiketal groups [28]. The diminishing difference in thermal stabilities of 3-tetraPCL1000-I to III could be due to a flowing transition from the structures I and II during the thermal treatment resulting 3-tetraPCL1000-III as the final and most stable polymer network structure.

### 3.2. Water-vs temperature-mediated dissociative mechanism

The polymers 3-tetraPCL1000-I, -II and III were subjected to solubility and swelling experiments in dry acetone aiming at elucidating the nature of the resulting polymer structures formed by chain elongation or crosslinking reaction. In dry acetone the polymer 3-tetraPCL1000-I swelled up to 286% of its original mass (Figure S 14, Supporting Information) pointing to crosslinked polymer structures. 3-tetraPCL1000-II swelled by 118% and reached its original volume retaining 90% of the original mass after drying for 12 h at 100 °C in vacuum. In a mixture of acetone and water (9: 1) 3-tetraPCL1000-I dissolved within 24 h in contrast to 3-tetraPCL1000-II/-III.

As described for other hemiketal based polymers, a competitive reaction with PCLs hydroxyl groups was assumed to take place entailing bond cleavage of 3-tetraPCL1000-I with the recovery of the starting

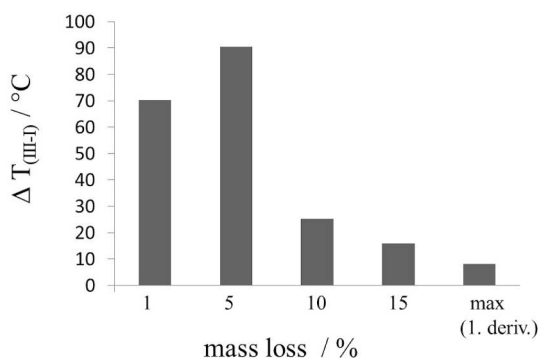


Fig. 7. Temperature differences of TGA measurements between the polymers 3-tetraPCL1000-I and 3-tetraPCL1000-III at 1%, 5%, 10, 15% and the maximum mass loss (maximum of the first derivative) under nitrogen atmosphere.

materials after drying in vacuum [21,28]. NMR-experiments confirmed the formation of bis(gem-diol) **2** and the polyester polyol tetraPCL1000 when depolymerizing 3-tetraPCL1000-I in DMSO- $d_6$  and water (9:1) (Fig. 8). Comparing reference NMR-spectra of bis(geminal-diol) **2** and tetraPCL1000 with the spectra of the depolymerized polymer, the formation of the bis(geminal-diol) **2** and tetraPCL1000 upon the alcohol-water exchange reaction was clearly demonstrated. The signals a and c with the chemical shift of  $\delta = 196.44$  ppm (a) and  $\delta = 196.38$  ppm (c) were assigned to the two carbonyl groups, and the one at  $\delta = 97.40$  ppm (b) to the quaternary carbon of the bis(geminal diol) **2**. The additional signal d at  $\delta = 100.47$  ppm indicates the presence of residual hemiketal bonds, which are linking single polyester polyols to dimers or oligomers.

Those solubility experiments proved that the presence of water leads to a dissociation of the polymer network based on 3-tetraPCL1000-I. The endothermic event observed in DSC experiments accompanying 3-tetraPCL1000-I pointed, however, to a thermally induced liquefying. To get a deeper insight the storage and loss modulus during cooling from 130 to 0 °C was determined (Fig. 9). At 130 °C 3-tetraPCL1000-I is liquid and exhibits a loss modulus surpassing the storage modulus. This is true for materials with a predominating viscous fraction over the elastic fraction [34]. The loss modulus equals the storage modulus at 80 °C and

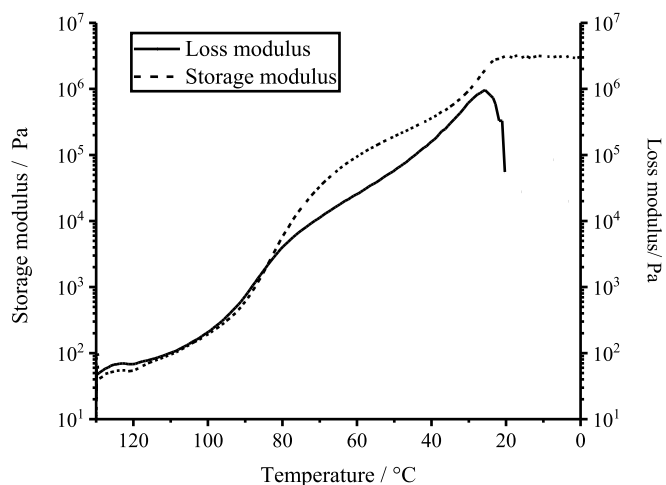


Fig. 9. Rheological examination of polymer network after processing condition I during a cooling process from 130 °C to 0 °C.

increases with decreasing temperature. Thus, the elastic ratio of the sample exceeds the viscous part below 80 °C. A large drop in the loss modulus at room temperature marks the glass transition region.

The results originating from water- and temperature mediated experiments with 3-tetraPCL1000-I indicate that reversible hemiketal linkages form a dissociative polymer network under mild processing conditions. S. Nakagawa et al. proposed two options for the depolymerization of hemiketal bonds. A thermally indicated elimination of alcohol from hemiketal and an exchange reaction with traces of water [29]. For both depolymerization cases, namely the water mediated and the thermally induced depolymerization, he assumed the exchange reaction with water being the main reason. NMR experiments with 3-tetraPCL1000-I proved a water-mediated depolymerization based on an exchange reaction with water (Fig. 8). However, in case of the thermally induced rheology experiment, we assume that the depolymerization is based on an equilibrium shift between the hemiketal compound, and the corresponding bistriketone **3** and polyester polyol rather than an exchange reaction with water. Most of the water was probably removed as

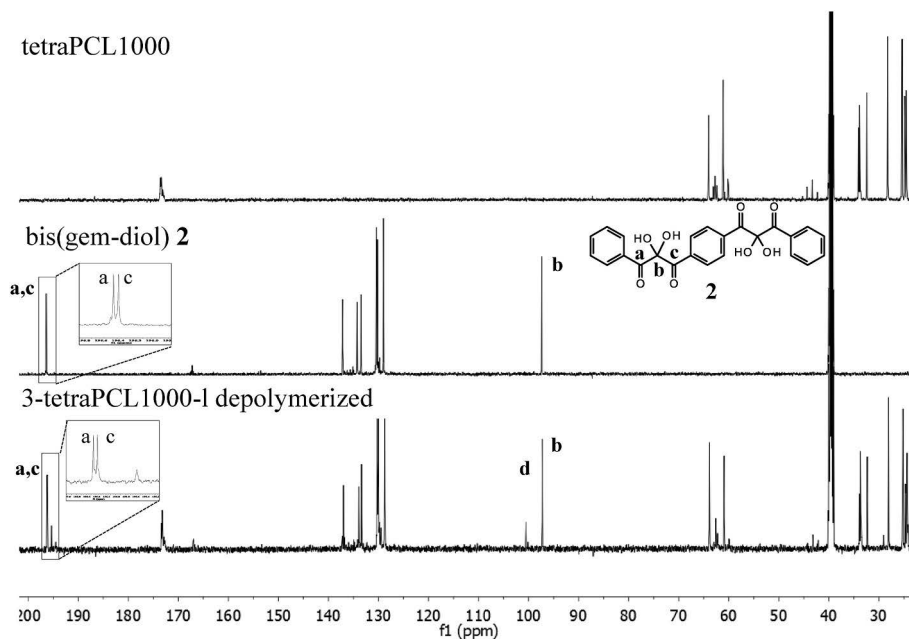


Fig. 8. NMR spectroscopic examination of the tetraPCL1000, the bis(geminal diol) **2** and the reaction mixture in deuterated DMSO and water (signal d indicates the presence of residual hemiketal bond).

the starting materials have been pre-dried and the crosslinking reaction was performed at 130 °C. Moreover, the samples were always stored in a desiccator with a relative humidity <2%.

For a better understanding of the temperature-mediated ketone/hemiketal formation a model hemiketal compound based on PEO (3-diPEO400-I) was used to avoid carbonyl group band overlap and studied by infrared spectroscopy. The reaction of PEO and bistriketone **3** was studied after hemiketal formation according to processing conditions I. Upon heating the sample to 80 °C, a signal at 1723 cm<sup>-1</sup> assigned to the central carbonyl group appeared and disappeared again during cooling indicating a shift of equilibrium. Thus, the central group in bistriketone was transformed from carbonyl to hemiketal forth and back in dependence of the temperature (Fig. 10 and for further information Figure S 16, Supporting Information). In case of an exchange reaction with water a germinal diol would be generated, which would lack tricarbonyl groups with a band at 1723 cm<sup>-1</sup>.

From the experiments one could conclude that below 80 °C bistriketone **3** and polyester polyols form hemiketal bond based crosslinks that decrosslink above a temperature of 80 °C due to a shift of the reaction equilibrium in direction of the dissociated state. Such materials are known to rearrange their topology very quickly due to the thermally induced temporary loss of crosslinking points, which is indicated by a rapid drop in viscosity. As a result of the cooling, the crosslinking points recover revealing unchanged physical properties compared to the starting polymer. This is a typical behavior that has been reported for dissociative networks [5]. This type of dynamic covalent bonding would allow for a thermally induced dissolution of thermosetting polymers and by this facilitating their recycling.

In contrast to 3-tetraPCL1000-I, polymers based on 3-tetraPCL1000-II did not dissolve in acetone/water mixtures within 24 h and the swelling factor of 3-tetraPCL1000-II is significantly lower indicating that a more stable network formed during elongated heating (processing condition II). As the *T<sub>g</sub>* did not change upon the processing procedure,

changes in the network density are not probable to be responsible for the changes in swelling and solubility behavior of 3-tetraPCL1000-II. Furthermore, that was confirmed by a gel contents of 80% determined in dry acetone and 67% in a acetone-water mixture (9:1) for 3-tetraPCL1000-II. The lower gel content in presence of water is probably due to residual hemiketal bonds present in the intermediate stage of that polymer network II.

Therefore, different strong nucleophiles were applied as possible reactants initiating cleavage of the network points. For this, 3-tetraPCL1000-II was treated with solutions of *n*-butylamine, 1-butanethiol, 4-nitrothiophenol, 4-nitrophenol, 1-butanol, 4-nitroaniline and water in NMP, respectively. A complete dissolution of 3-tetraPCL1000-II after 24 h was solely observed in case of *n*-butylamine. All other tested nucleophiles did not dissolve but entailed swelling of the polymer sample (Figure S 15, Supporting Information). The reactivity of *n*-butylamine can be explained mainly with its nucleophilicity rather than basicity as the base sodium hydroxide did not entail dissolution. Secondly, the polymer network 3-tetraPCL1000-III after processing condition III was successfully dissolved with *n*-butylamine as well. Those experiments proved that the covalent polymer networks after processing stage II and III are still dynamic enough to react with a strong nucleophile as a reactive solvent. They are, however, resistant to organic solvents and weaker nucleophiles such as water. Further investigations need to be performed to elucidate the chemical structure being formed throughout the processes and changing the nature of the network.

### 3.3. Nature of polymer network affecting material properties

The dissociative nature of the polymer network gives reason to assume self-healing properties of hemiketal based polymers. The crosslinked polymer 3-tetraPCL1000-I was cut with a scalpel into two pieces that were then recombined and exposed to 130 °C for 6 min to trigger the dynamic covalent chemistry by dissociation mechanism. The heated

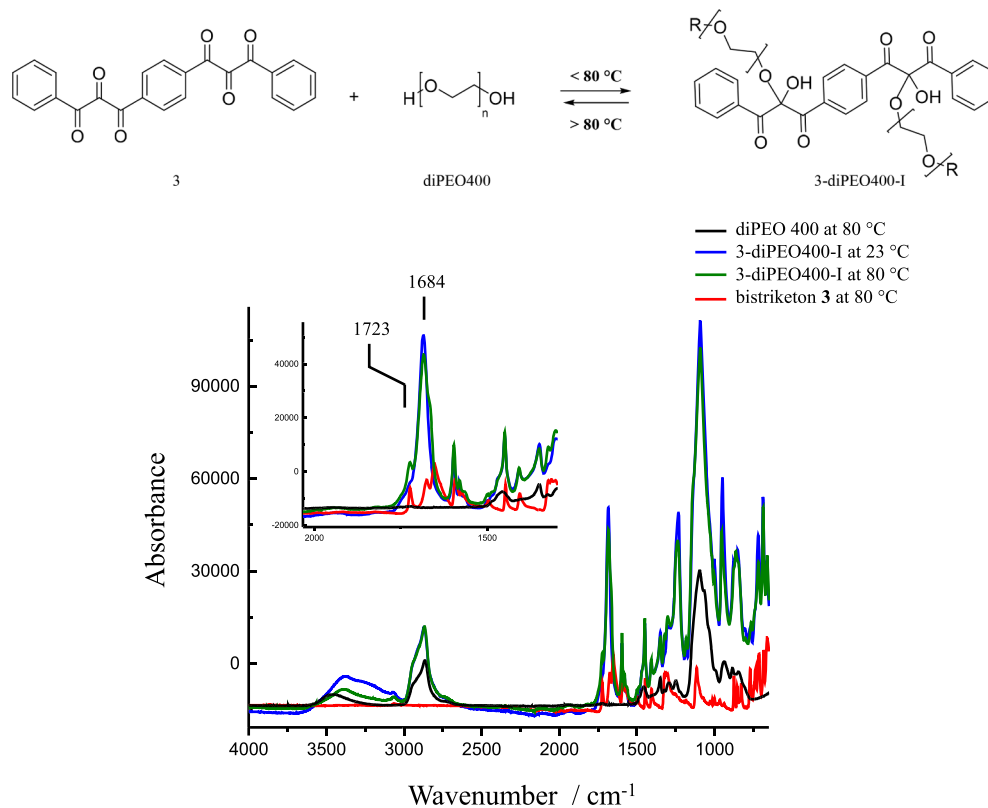


Fig. 10. top) Reaction scheme of **3** and diPEO400 yielding 3-diPEO400-I; bottom). ATR IR analyse of diPEO400 and 3-diPEO400-I, bistriketone **3** at 80 °C and 3-diPEO400-I at 23 °C.

part of the sample liquefied, changed the color from orange to red with a subsequent closing of the gap. After cooling, the original fracture disappeared (Fig. 11).

In order to investigate the material properties before damage and after self-healing, test specimens of 3-tetraPCL1000-I were analyzed, and fractured in tensile tests with subsequent self-healing, and testing after each self-healing cycle. For all samples a sharp increase in stress followed by an abrupt decrease was observed. Afterwards, the material started to elongate extensively and showed cold drawing before failure (Fig. 12). A reason for that behavior could be the testing temperature of 23 °C, which is in the  $T_g$  region of the material [35]. A further reason could be the high testing speed of 200 mm/min.

After self-healing, the material integrity of all samples ( $n = 9$ ) was successfully restored and its behavior during tensile testing did not change with the healing cycles. The observation that the specimens failed at different locations in the test specimen in the repeated load tests (breaking points) confirmed that the self-healing is effective. Nevertheless, a slight decrease of mechanical properties was observed with each healing cycle (Figure S 17, Supporting Information). On the one hand, this could be related to the sample quality. During the self-healing process, void formation was observed, which leads to porosity and thus to predetermined breaking points in the material. On the other hand, further (side) reactions could be initiated with each heating cycle of the self-healing changing the materials mechanical properties.

### 3.4. Adjusting mechanical properties by varying the polymer backbone

Thermal analysis by DSC showed that the  $T_g$  values did not vary with the processing conditions. With the aim to influence mechanical properties, crosslinking densities were adjusted by varying OH functionality, molar mass and stoichiometric ratio of **3** to the appropriate polyester polyol. The starting materials were processed with processing condition II to appropriate polymer networks, which were studied by DSC. In order to determine the effect of functionality on  $T_g$  evolution upon crosslinking, the number of hydroxyl groups was varied by using di, tri and tetra hydroxyl functionalized PCL oligomers with a molar mass of approx. 1000 g/mol (Figure S 18, Table S 1, Supporting Information). With an increasing number of hydroxyl groups the  $T_g$  of the crosslinked PCLs increased from -33 °C for the difunctional PCL (3-diPCL1000-II) to 10 °C in case of the tetrafunctional one (3-tetraPCL1000-II). A higher crosslinking density results from a higher number of available hydroxyl groups upon the reaction with the crosslinking agent **3**. The reaction of di-functionalized PCL oligomers (diPCL1000) with **3** resulted a chain elongation instead of a crosslinking which explains the low  $T_g$  of -33 °C.

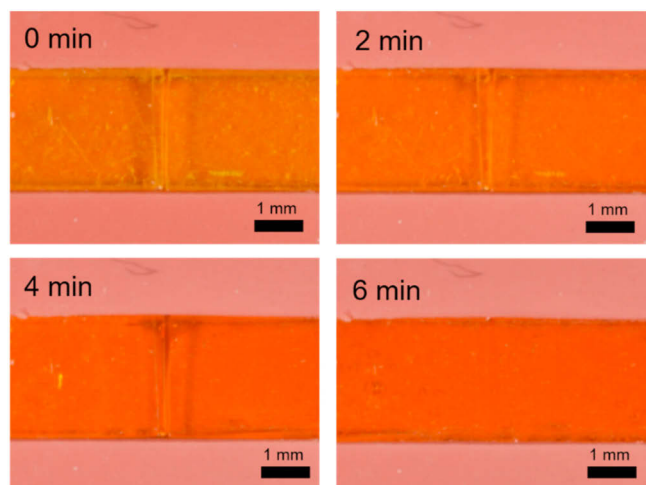


Fig. 11. Self-healing of the polymer network 3-tetraPCL1000-I at 130 °C after cut.

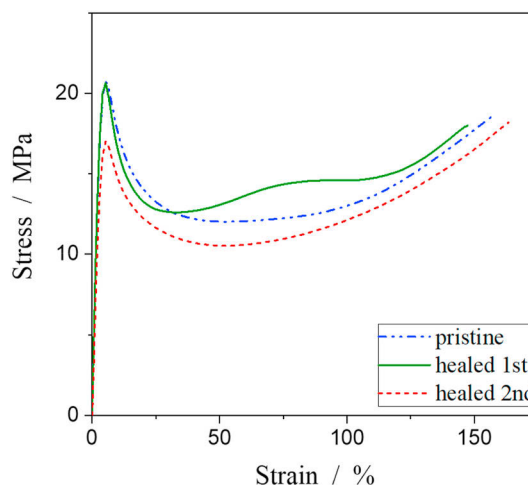


Fig. 12. Stress-strain curve of the polymer network 3-tetraPCL1000-I of one test specimen in a cyclic self-healing experiment.

A similar  $T_g$  behavior was observed if the molar mass of a trifunctional PCL was varied from 300 to 2000 g/mol (Figure S 19, Supporting Information). Crosslinking with **3** resulted polymers differing in the mean molar mass between the net points ( $M_c$ ). Thus, the lower the  $M_c$  value, the higher the measured  $T_g$ . Crosslinking of a triPCL300 yielded the highest  $T_g = 38$  °C, whereas triPCL2000 resulted a decrease in  $T_g$  down to -35 °C.

In a last condition, the influence of the stoichiometric ratio of the crosslinking compound **3** to the tetrafunctional PCL1000 on the  $T_g$  was studied (Fig. 13). The stoichiometric ratio required for a complete reaction is represented by 2 mol of **3** (two reactive functional groups) and 1 mol of tetraPCL1000 (four reactive functional groups). The crosslinked polymer generated at stoichiometric ratio a  $T_g$  of 10 °C. With an increasing content of the thermoplastic in the reaction mixture, the  $T_g$  values decreased yielding  $T_g = -30$  °C in case of 2 mol **3** (two reactive functional groups) per 2 mol PCL (four reactive functional groups) for a  $n_3/n_{PCL}$  ratio of 1. This could be explained by the lower crosslinking density or just chain elongation and thus, higher amount of thermoplastic parts in the material. Changing the stoichiometry by increasing the amount of the crosslinking molecule **3**, increased the  $T_g$  to a value around 2 °C. Further addition of the crosslinking agent, however, did not entail a further increase in  $T_g$  for the tetrafunctional PCL. Thus, reactions performed at stoichiometric ratio yielded the highest crosslinking density followed by the highest  $T_g$ .

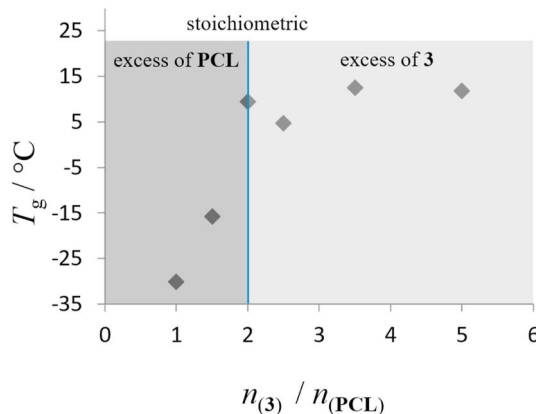


Fig. 13. Glass transition temperature of 3-tetraPCL1000 in dependence of molar ratio by the reaction of **3** with tetraPCL1000 (molar ratio of 2 = stoichiometric).

## 4. Conclusions

Polyester polyols were successfully crosslinked in a ketone/hemiketal reaction with the crosslinking molecule bistriketone **3** without the need of solvents, which opens further processing opportunities. Depending on the processing conditions, such as time and temperature, the resulting polymer networks differed in their thermal behavior, swelling, and solubility properties. At the same time,  $T_g$  values did not change pointing to steady overall network densities. Spectroscopic analysis proved that hemiketal bond formation yields dissociative polymer networks in solid state and under mild conditions that could be crosslinked and decrosslinked with water due to the reversible ketone/hemiketal reaction. The dissociative nature causes a liquefaction of the hemiketal network at temperatures above 80 °C and solidification again at temperatures below 80 °C. It has been proven that this behavior occurs through a shift in equilibrium between hemiketal and carbonyl/OH groups. Furthermore, the material showed self-healing properties stimulated by temperature. Mechanical testing proved that the sample performance is reproducible for at least two self-healing cycles.

However, longer processing and treatment at elevated temperature caused structural changes from hemiketal bonds to ester like bonding motifs yielding insoluble materials. That polymer structure did not become a liquid at elevated temperature and did not dissolve in organic solvent except for strong nucleophiles such as butylamine as a reactive solvent. Processing conditions II and III seem to affect and change the dissociative polymer network processed with milder conditions (processing conditions I).

Mechanical properties of the reversibly crosslinked polyesters could be adjusted by variations in the number of available OH-groups, the molar mass between crosslinks and the stoichiometric ratio during reaction of PCL and bistriketone **3**. Decreasing PCLs molar mass or increasing the number of OH-groups, provided polymers with a higher crosslinking density and therefore a higher  $T_g$ . Studies regarding the stoichiometry showed that the highest crosslinking density and the highest  $T_g$  were reached at stoichiometric ratio. Further investigations are ongoing regarding the dynamic and reversible character of the thermosetting material based on ketone/hemiketal chemistry.

## 5. Patents

This approach was registered as an invention to the European Patent Office (PCT/EP2019/052327). The international research report already recognizes the novelty and inventive condition. We are currently considering a number of citations when filing a patent.

## Funding

This research was funded by Bundesministerium für Bildung und Forschung, grant number 03XP0001.

## CRedit authorship contribution statement

**Tobias Urbaniak:** Conceptualization, Data curation, Investigation, Methodology, Writing – original draft. **Katrin Greta Hoffmann:** Investigation, Visualization. **Matthias Herrera Glomm:** Investigation, Visualization. **Hartmut Oschkinat:** Resources, Supervision. **Peter Schmieder:** Investigation. **Katharina Koschek:** Conceptualization, Funding acquisition, Project administration, Supervision, Writing – review & editing.

## Declaration of competing interest

The authors declare that they have no known competing financial interests or personal relationships that could have appeared to influence the work reported in this paper.

## Acknowledgments

Tobias Urbaniak thanks Nils Trieloff for technical support with solution NMR measurements.

## Appendix A. Supplementary data

Supplementary data to this article can be found online at <https://doi.org/10.1016/j.polymer.2021.123986>.

## References

- [1] N. Sowan, C.N. Bowman, L.M. Cox, P.K. Shah, H.B. Song, J.W. Stansbury, Dynamic covalent chemistry at interfaces: development of tougher, healable composites through stress relaxation at the resin–silica nanoparticles interface, *Adv. Mater. Inter.* 18 (2018) 1–21, <https://doi.org/10.1002/admi.201800511>.
- [2] Z. Wei, J.H. Yang, J. Zhou, F. Xu, M. Zrinyi, P.H. Dussault, et al., Self-healing gels based on constitutional dynamic chemistry and their potential applications, *Chem. Soc. Rev.* 23 (2014) 8114–8131, <https://doi.org/10.1039/C4CS00219A>.
- [3] C.L. Lewis, E.M. Dell, A review of shape memory polymers bearing reversible binding groups, *J. Polym. Sci., Part B: Polym. Phys.* 54 (2016) 1340–1364, <https://doi.org/10.1002/polb.23994>.
- [4] C.J. Kloxin, C.N. Bowman, Covalent adaptable networks, *Chem. Soc. Rev.* 17 (2013) 7161–7173, <https://doi.org/10.1039/C3CS60046G>.
- [5] W. Denissen, J.M. Winne, F.E. Du Prez, *Vitrimers*, *Chem. Sci.* 1 (2016) 30–38, <https://doi.org/10.1039/c5sc02223a>.
- [6] C.N. Bowman, C.J. Kloxin, Covalent adaptable networks: reversible bond structures incorporated in polymer networks, *Angew. Chem. Int. Ed.* 18 (2012) 4272–4274, <https://doi.org/10.1002/anie.201200708>.
- [7] K. Ishida, V. Weibel, N. Yoshie, Substituent effect on structure and physical properties of semicrystalline Diels–Alder network polymers, *Polymer* 13 (2011) 2877–2882, <https://doi.org/10.1016/j.polymer.2011.04.038>.
- [8] N. Yoshie, S. Saito, N. Oya, A thermally-stable self-mending polymer networked by Diels–Alder cycloaddition, *Polymer* 26 (2011) 6074–6079, <https://doi.org/10.1016/j.polymer.2011.11.007>.
- [9] W. Denissen, G. Rivero, R. Nicolay, L. Leibler, J.M. Winne, F.E. Du Prez, Vinylogous urethane vitrimers, *Adv. Funct. Mater.* 16 (2015) 2451–2457, <https://doi.org/10.1002/adfm.201404553>.
- [10] W. Denissen, I. de Baere, W. van Paepegem, L. Leibler, J. Winne, F.E. Du Prez, Vinylogous urea vitrimers and their application in fiber reinforced composites, *Macromolecules* 5 (2018) 2054–2064, <https://doi.org/10.1021/acs.macromol.7b02407>.
- [11] G.A. Barcan, X. Zhang, R.M. Waymouth, Structurally dynamic hydrogels derived from 1,2-dithiolanes, *J. Am. Chem. Soc.* 17 (2015) 5650–5653, <https://doi.org/10.1021/jacs.5b02161>.
- [12] A. Rekondo, R. Martin, A. Ruiz de Luzuriaga, G. Cabañero, H.J. Grande, I. Odriozola, Catalyst-free room-temperature self-healing elastomers based on aromatic disulfide metathesis, *Mater. Horiz.* 2 (2014) 237–240, <https://doi.org/10.1039/C3MH00061C>.
- [13] A. Ruiz de Luzuriaga, R. Martin, N. Markaide, A. Rekondo, G. Cabañero, J. Rodríguez, et al., Epoxy resin with exchangeable disulfide crosslinks to obtain reprocessable, repairable and recyclable fiber-reinforced thermoset composites, *Mater. Horiz.* 3 (2016) 241–247, <https://doi.org/10.1039/C6MH00029K>.
- [14] T. Ono, T. Nobori, J.-M. Lehn, Dynamic polymer blends—component recombination between neat dynamic covalent polymers at room temperature, *Chem. Commun.* 12 (2005) 1522–1524, <https://doi.org/10.1039/B418967A>.
- [15] P. Taynton, Development of Polyimine-Based Dynamic Covalent Networks: from Malleable Polymers to High-Performance Composites, Dissertation, Santa Cruz, California, 2015.
- [16] P. Taynton, C. Zhu, S. Loob, R. Shoemaker, J. Pritchard, Y. Jin, et al., Re-healable polyimine thermosets: polymer composition and moisture sensitivity, *Polym. Chem.* 46 (2016) 7052–7056, <https://doi.org/10.1039/C6PY01395C>.
- [17] P. Taynton, K. Yu, R.K. Shoemaker, Y. Jin, H.J. Qi, W. Zhang, Heat- or water-driven malleability in a highly recyclable covalent network polymer, *Adv. Mater.* 23 (2014) 3938–3942, <https://doi.org/10.1002/adma.201400317>.
- [18] P. Taynton, H. Ni, C. Zhu, K. Yu, S. Loob, Y. Jin, et al., Repairable woven carbon fiber composites with full recyclability enabled by malleable polyimine networks, *Adv. Mater.* 15 (2016) 2904–2909, <https://doi.org/10.1002/adma.201505245>.
- [19] T. Urbaniak, M. Soto, M. Liebecke, K. Koschek, Insight into the mechanism of reversible ring-opening of 1,3-benzoxazine with thiols, *J. Org. Chem.* 8 (2017) 4050–4055, <https://doi.org/10.1021/acs.joc.6b02727>.
- [20] A.W. Kawaguchi, A. Sudo, T. Endo, Polymerization–depolymerization system based on reversible addition–dissociation reaction of 1,3-benzoxazine with thiol, *ACS Macro Lett.* 1 (2013) 1–4, <https://doi.org/10.1021/mz3005296>.
- [21] T. Yuki, M. Yonekawa, K. Matsumoto, I. Tomita, T. Endo, Construction of reversible crosslinking–decrosslinking system consisting of a polymer bearing vicinal tricarbonyl structure and poly(ethylene glycol), *Polym. Bull.* 2 (2016) 345–356, <https://doi.org/10.1007/s00289-015-1490-5>.
- [22] T. Dei, K. Morino, A. Sudo, T. Endo, Synthesis and reversible hydration–dehydration system of copolymers bearing a vicinal tricarbonyl structure, *J. Polym. Sci. Polym. Chem.* 13 (2012) 2619–2625, <https://doi.org/10.1002/pola.26035>.

- [23] K. Morino, A. Sudo, T. Endo, Reversible fixation and release of alcohols by a polymer bearing vicinal tricarbonyl moieties and its application to synthesis and reversible cross-linking–de-cross-linking system of a networked polymer, *Macromolecules* 11 (2012) 4494–4499, <https://doi.org/10.1021/ma3003196>.
- [24] T. Dei, K. Morino, A. Sudo, T. Endo, Construction of reversible hydration–dehydration system by a model compound and a novel polymer bearing vicinal tricarbonyl structure, *J. Polym. Sci. Polym. Chem.* 10 (2011) 2245–2251, <https://doi.org/10.1002/pola.24656>.
- [25] M. Regitz, H.-G. Adolph, Untersuchungen an Diazoverbindungen, IV1) Vicinale Tricarbonylverbindungen aus 2-Diazo-1,3-dicarbonyl-Verbindungen durch Sauerstoff-Halogen-Insertion, *Justus Liebigs Ann. Chem.* 1 (1969) 47–60, <https://doi.org/10.1002/jlac.19697230107>.
- [26] T. Yuki, M. Yonekawa, K. Matsumoto, Y. Sei, I. Tomita, T. Endo, Hemithioketal formation of vicinal tricarbonyl compound with thiols and their recovery, *Tetrahedron* 32 (2016) 4783–4788, <https://doi.org/10.1016/j.tet.2016.06.034>.
- [27] T. Yuki, M. Yonekawa, Y. Furusho, Y. Sei, I. Tomita, T. Endo, Reversible capture and release of aromatic amines by vicinal tricarbonyl compound, *Tetrahedron* 22 (2016) 2868–2873, <https://doi.org/10.1016/j.tet.2016.03.093>.
- [28] M. Yonekawa, Y. Furusho, T. Takata, T. Endo, Reversible crosslinking and decrosslinking of polymers containing alcohol moiety using an acyclic bifunctional vicinal triketone, *J. Polym. Sci., Part A: Polym. Chem.* 7 (2014) 921–928, <https://doi.org/10.1002/pola.27087>.
- [29] S. Nakagawa, S. Nakai, K. Matsuoka, N. Yoshie, Alcohol-assisted self-healing network polymer based on vicinal tricarbonyl chemistry, *Polymer* (2019) 101–108, <https://doi.org/10.1016/j.polymer.2018.11.061>.
- [30] M. Yonekawa, Y. Furusho, Y. Sei, T. Takata, T. Endo, Synthesis and X-ray structural analysis of an acyclic bifunctional vicinal triketone, its hydrate, and its ethanol-adduct, *Tetrahedron* 20 (2013) 4076–4080, <https://doi.org/10.1016/j.tet.2013.03.065>.
- [31] J. Cavanagh, *Protein NMR Spectroscopy: Principles and Practice*, first ed, Elsevier professional, 1995 s.l.
- [32] A. Pines, M.G. Gibby, J.S. Waugh, Proton-enhanced nuclear induction spectroscopy. A method for high resolution NMR of dilute spins in solids, *J. Chem. Phys.* 4 (1972) 1776–1777, <https://doi.org/10.1063/1.1677439>.
- [33] B.M. Fung, A.K. Khitrin, K. Ermolaev, An improved broadband decoupling sequence for liquid crystals and solids, *J. Magn. Reson. (San Diego, Calif)* 1 (1997) 97–101, <https://doi.org/10.1006/jmre.1999.1896>, 2000.
- [34] T. Defize, J.-M. Thomassin, M. Alexandre, B. Gilbert, R. Riva, C. Jérôme, Comprehensive study of the thermo-reversibility of Diels–Alder based PCL polymer networks, *Polymer* (2016) 234–242, <https://doi.org/10.1016/j.polymer.2015.11.055>.
- [35] C. Walters, D. Ballesteros, V.A. Vertucci, Structural mechanics of seed deterioration: standing the test of time, *Plant Sci.* 6 (2010) 565–573, <https://doi.org/10.1016/j.plantsci.2010.06.016>.